Earth System Dynamics

Discussions

Open Access

The impact of land cover generated by a dynamic vegetation model on climate over East Asia in present and possible future climate

M.-H. Cho[1], K.-O. Boo[2], G. M. Martin[3], J. Lee[2], and G.-H. Lim[1]

[1]School of Earth and Environmental Sciences, Seoul National University, Seoul, Republic of Korea
[2]National Institute of Meteorological Research, Korea Meteorological Administration, Jeju, Republic of Korea
[3]Met Office Hadley Centre, FitzRoy Road, Exeter, UK

Correspondence to: M.-H. Cho (mhjo77@snu.ac.kr)

Title Page

Abstract	Introduction
Conclusions	References
Tables	Figures

|◄ | ►|

◄ | ►

Back | Close

Full Screen / Esc

Printer-friendly Version

Interactive Discussion

Abstract

This study investigates the impacts of land cover change, as simulated by a dynamic vegetation model, on the summertime climatology over Asia. The climate model used in this study has systematic biases of underestimated rainfall around Korea and over-
5   estimation over the South China Sea. When coupled to a dynamic vegetation model, the resulting change in land cover is accompanied by an additional direct radiative effect over dust-producing regions. The direct radiative effect of the additional dust contributes to increasing the rainfall biases, while the land surface physical processes are related to local temperature biases such as warm biases over North China. In
10 time-slice runs for future climate, as the dust loading changes, anomalous anticyclonic flows are simulated over South China Sea, resulting in reduced rainfall over the South China Sea and more rainfall toward around Korea and South China. In contrast with the rainfall changes, the influence of land cover change and the associated dust radiative effects are very small for future projection of temperature, which is dominated by atmo-
15 spheric CO_2 increase. The results in this study suggest that the land cover simulated by a dynamic vegetation model can affect, and be affected by, model systematic biases on regional scales over dust emission source regions such as Asia. In particular, analysis of the radiative effects of dust changes associated with land cover change is important in order to understand future changes of regional precipitation in global warming.

1   Introduction

20 Bordered by the Tibetan Plateau to the west, the Eurasian land mass to the north-west, and the vast Pacific Ocean to the south and east, East Asia has experienced one of the most pronounced monsoon climates of the globe for centuries (Lau and Li, 1984). Land surface properties are important because of their known impact on
25 the East Asian monsoon circulation (Kang and Hong, 2008; Lee et al., 2011) and on the Indian monsoon (Douglas et al., 2006; Lee et al., 2009; Bayer et al., 2012; Martin

and Levine, 2012). Lee et al. (2011) proposed that a replacement of vegetation with bare soil would cause an associated decrease in latent heat during the summer, which could weaken East Asian monsoon circulation. This decrease in latent heat flux over land could weaken the East Asian monsoon via a positive feedback between the latent heat flux contrast and rainfall. Yamashima et al. (2011) showed a similar study over the Indian subcontinent and Southeastern China. Land surface property changes from forest to cultivated land have resulted in a decrease in the monsoon rainfall and provoked an associated weakening of the Asian summer monsoon circulation. Moreover, there are a few studies investigating the influence of land cover change that have demonstrated significant impact on East Asian Monsoon (Kang et al., 2005), but they usually used satellite-based (Suh and Lee, 2004; Kang and Hong, 2008) and idealized land cover change (Lee et al., 2011).

Although Earth System models with dynamic vegetation schemes allow representation of the carbon cycle feedbacks on climate, the land cover distribution could also be influenced by, and indeed influence, model systematic biases (Martin and Levine, 2012, hereafter ML12). Land surface property changes have effects on the atmosphere through physical processes (such as changes in surface roughness, albedo and evapotranspiration), and can induce additional indirect impacts when coupled with aerosol processes as well. For example, changes in surface emissions of mineral dust that are caused by changes in bare soil fraction will have a radiative effect in the atmosphere. Additional dust loading of the atmosphere resulting from land cover change in an Earth System model could, therefore, add to the model uncertainty via feedbacks with model systematic biases such as lack of rainfall over dust-producing regions. Dust affects both shortwave and longwave radiative fluxes, and the effects of mineral dust on the radiation budget are important due to the widespread distribution and large optical depth of mineral dust (Sokolik and Toon, 1996). A study by Yoshioka et al. (2007) suggests that the direct radiative forcing of dust can explain up to 30 % of the observed precipitation reduction in the Sahel in three decadal scale simulation. Dust is removed from the atmosphere by both dry and wet deposition processes, providing a source of iron

to phytoplankton and thus potentially affecting the carbon cycle (Collins et al., 2011). Since Northeast Asia is one of the major dust emission source regions, land surface property changes over this source region need to be studied. Aerosol, as one of the fundamental atmospheric constituents, has an important impact on the climate sys-
tem. Ramanathan et al. (2005) showed that global dimming causes a long-term (multi-decadal) weakening of the South Asian monsoon by reducing the meridional surface temperature gradient between the Asian land mass and the Indian Ocean. Aerosol affects precipitation events through cloud physics processes in China (Qian et al., 2009), while dust can also contribute to Asian monsoon rainfall anomalies by heating the up-
per troposphere (Lau et al., 2006; Lau and Kim, 2006). Therefore, aerosol impacts due to land cover changes may be important in regional climate over East Asia.

ML12 investigated land surface and dust impacts in terms of the feedback between model systematic biases. Their results reflect that over dust producing regions, land cover change simulated by a Dynamic Global Vegetation Model (DGVM) can affect
both the present-day simulation and the future response as well. According to Hurrel et al. (2009) and McCarthy et al. (2012), since model systematic biases affect climate model sensitivity, we need to study processes related to systematic biases in order to understand future climate projections. Motivated by ML12, this study extends ML12 by applying their results for East Asia. The aims of this study are: first, to investigate
the physical influence of land cover conditions and associated aerosol loading on the rainfall and surface temperature over East Asia; and second, to provide insight into the contribution of uncertainty in modeling of land cover changes to the uncertainty in future climate projections of rainfall land surface temperature for the region.

The present paper is organized as follows. Section 2 briefly describes the global
circulation model used in this study, the experimental design, and the data. The results of the study are given in Sect. 3. The impact of land cover distribution and radiative effect of dust under present and possible future climate are all provided in this section. A summary and discussion are given in Sect. 4.

2   Model experimental design and data

In this study, we used the ML12 datasets which were performed using the Hadley Centre Global Environmental Model version 2 (HadGEM2) model family that had been developed by the UK Met Office (The HadGEM2 Development Team, 2011). The horizontal grid interval was $1.25° \times 1.875°$ in the latitude–longitude directions, and 38 vertical layers were used with the top of atmosphere over 39 km in height. The land surface scheme in the HadGEM2 family is a tiled version of the Met Office Surface Exchange Scheme (MOSES) version 2, which represents heterogeneous surface properties (Cox et al., 1999; Essery and Clark, 2003). A grid box represents a mixture of five vegetation or plant-functional types (PFTs), which include broadleaf trees, needleleaf trees, temperate C_3 grass, tropical C_4 grass, and shrubs, and four non-vegetated surface types, which include urban, inland water, bare soil, and ice. Surface fluxes and temperatures are calculated separately for each surface type and are aggregated according to each tile's fractional coverage before being passed to the atmospheric model (Lawrence and Slingo, 2004).

The experiment configuration is as follows. For the present-day (1980–2005) runs, the HadGEM2 atmosphere-only model was forced with observed sea surface temperatures (SSTs) and sea ice. The experimental design and forcing datasets are as specified by the Fifth Coupled Model Intercomparison Project (CMIP5; Taylor et al., 2012) and are detailed in Taylor et al. (2012). The land cover and vegetation types were prescribed by the International Geophysical Biophysical Programme (IGBP; Loveland et al., 2000) with a prescribed seasonally-varying leaf area index (LAI) based on Moderate Resolution Imaging Spectroradiometer (MODIS) Terra Collection 5 monthly LAI datasets. Historical land use change information based on CMIP5, provided to CMIP5 by the Land Use Harmonization team (Hurtt et al., 2011), were applied by Baek et al. (2013) to the IGBP land cover data in order to prescribe time-varying land cover fields for HadGEM2-A. This is referred to as the "A" experiment.

For the future timeslice experiments, the atmosphere component is forced with CO_2 and trace gases for the year 2100 based on the Representative Concentration Pathway (RCP) 8.5 scenario of the CMIP5. The SSTs were obtained by applying the difference between 30 year mean SSTs centred around 2100 (from the HadGEM2 Earth System (HadGEM2-ES) RCP8.5 scenario coupled model run) and 30 years mean SSTs centred around 1990 (from the HadGEM2-ES historical run), to the present-day monthly-varying observed SSTs from 1980–2005. The projected future land use changes for the period 2080–2110 based on CMIP5 RCP8.5 scenarios were applied in order to prescribe time-varying land cover fields for HadGEM2-A timeslice experiment. This is referred to as the "Ats" experiment.

In addition to the "A" and "Ats" experiments, alternative representations of global vegetation cover from a DGVM were used as the land cover component for further HadGEM2-A experiments under present-day and future climates. In these experiments, the monthly mean land cover information from the HadGEM2-ES historical and RCP8.5 runs are used in HadGEM2-A in place of the standard land cover distribution as described above. The HadGEM2-ES configuration uses the Top-down Representation of Interactive Foliage and Flora Including Dynamics (TRIFFID) dynamic vegetation model (Cox, 2001) to simulate the land cover changes from the pre-industrial control period through the present-day and into the future following the CMIP5 RCP scenarios, and land use changes from Hurtt et al. (2011) are applied as disturbances (see Jones et al., 2011 for more details). Therefore, in these additional experiments, the variations in land cover with time during these periods in HadGEM2-ES are experienced by HadGEM2-A, but there is no interactive terrestrial carbon cycle and no feedbacks on the land cover. Variations in land cover from years 1980–2005 of HadGEM2-ES are used in the present-day experiment of this type, referred to as "AE", while the variations in land cover from years 2080–2110 of HadGEM2-ES are applied to the future timeslice experiment denoted "AEts".

According to ML12, the AE experiment shows a large increase in dust, which is generated as a result of the additional fraction of bare soil occurring in HadGEM2-ES as

a result of the feedback between the interactive vegetation and the model's systematic rainfall biases in dust-producing regions. To evaluate the radiative effects of the dust, an additional pair of experiments was carried out where the direct radiative effects of the dust were switched off. These experiments have the suffix "nod" meaning "no dust radiative effects". Therefore, "Anod" means a HadGEM2-A simulation with the standard land cover distribution in the present-day, "AEnod" means a HadGEM2-A present-day simulation with HadGEM2-ES land cover without the direct radiative effects of the dust, and "AEnodts" means a HadGEM2-A future timeslice simulation with HadGEM2-ES land cover without the direct radiative effects of dust. The total experiments are listed in Table 1.

To compare model results in the present-day runs with observations we used the Global Precipitation Climatology Project (GPCP) precipitation (Alder et al., 2003; Huffman et al., 2009), the CPC Merged Analysis of Precipitation (CMAP, Xie and Arkin, 1997) and the Climatic Research Unit (CRU) mean surface air temperature (Harris et al., 2013). In this study, summer represents the period from June to August.

3   Modeling results

3.1   Present day

3.1.1   Impact of ES land cover on average temperature and precipitations

First we examine summer precipitation over East Asia. Figure 1a shows the typical summertime precipitation distribution of the East Asian summer monsoon. The summer monsoon rainy season evolves with the rainband development covering South China, Korea, Japan and the adjacent seas. Formation of frontal systems is associated with the North Pacific Subtropical High and southwesterlies over the South China Sea. The rainband region, in contrast with the equatorial region, has a small observational uncertainty (Fig. 1b). In Fig. 2, we analyze the North China (NC) region (35–50° N,

105–120° E), Korea (KR) 25–40° N, 120–135° E, and South China (SC) region (20–35° N, 105–120° E), which together represent a large contrast in land cover distribution over East Asia. Simulated precipitation compared with observation (GPCP precipitation) shows a systematic bias in Fig. 2. Precipitation is underestimated over the KR area and overestimated over SC. These spatial features remain in AE, although the underestimated rainfall over KR become larger in AE than A.

Figure 3 represents summer surface air temperature bias in the model results compared with the CRU observation data. There is a warm bias greater than 1 K in NC and KR, but only a small bias in SC (Fig. 3a). The warm bias over KR is slightly smaller in AE compared to A (Fig. 3c and d). In order to shed light on the bias changes on the regional scale, the land cover difference between AE and A is examined (Fig. 4). Among the five vegetation and bare soil surface types over East Asia, the largest changes are in broadleaf, C_3 grass and bare soil types. Over North China, the increase in bare soil fraction is large. This unrealistic high bare soil fraction has an impact on high dust emission over this region because dust is only emitted from the bare soil fraction of a grid box in this model. In contrast, the South China region is covered by larger broadleaf fraction (Fig. 4) in the AE compared with A, replacing bare soil, shrub and needle-leaf tree. To the north of 50° N, the increase in shrub fraction is distinct (also seen in Fig. 5 of ML12).

ML12 showed that bare soil area expansion from the changes in the vegetation distribution between AE and A generates additional dust, resulting in a substantial direct radiative impact on the Indian monsoon rainfall. They suggest separate analysis for the dust radiative feedback from the response to land cover change. Accordingly, we examine experiments Anod and AEnod (see Table 1).

In Fig. 2, a marked precipitation underestimation over KR is shown compared with observations, particularly when the ES land cover is used. The dry bias amplitudes in summer become larger in AE compared with A (Fig. 2). To estimate the radiative effect of dust on rainfall when the HadGEM2-ES land cover distribution was used, AE was compared with AEnod. The dry bias amplitude of AE decreases in AEnod (Fig. 5) but

is still slightly larger than in A. Thus the radiative effect of dust reinforces the dry bias in the KR region (compare Fig. 2b and d with Fig. 5). This is consistent with the results of ML12 for the South Asian region.

To examine the dust radiative effect and land cover change effect in detail, the dry bias in summer over KR in Figs. 2 and 5 is considered using Fig. 6. The pattern of changes between "AE – A" in Fig. 6a is similar to the "AE – AEnod" changes (Fig. 6c) rather than those of "AEnod – Anod" (Fig. 6b). This suggests that the radiative effects of changes in dust that are associated with the land cover changes are likely to be more important for simulating precipitation over East Asia than the changes in surface processes associated with the same land cover changes.

In Fig. 7 we make a similar comparison for surface air temperature changes. We find that the dust radiative effect on surface air temperature is associated with a small widespread cooling (Fig. 7c), whereas the surface process effects of the land cover change are associated with a more substantial warming/cooling pattern across the region, as shown in the AEnod – Anod (Fig. 7b) and AE – A (Fig. 7a) differences. Over northeastern Eurasia, the increase of shrub fraction replacing broadleaf and needleleaf trees shows a distinct cooling of surface air temperature induced from an increase of surface albedo.

3.1.2 Impact of changes in land cover with no dust radiative feedback

To understand more clearly the impacts of the changes in the vegetation distribution in Fig. 7a and b, we examined the climate response without the direct radiative effect of dust. The aforementioned increase in warm bias over NC "AEnod–Anod" (Fig. 7b) is considered. Over NC, as the bare soil fraction is larger in AE than A (Figs. 4f and 8a, b), the roughness length reduces while soil evaporation and canopy evaporation decrease. Reduced roughness length induces a decrease of sensible and latent heat fluxes from the surface to the atmosphere (Fig. 8c, d and f). The decrease in latent heat flux is associated with reduced cloud amount (Fig. 8e), as well as being favorable for surface warming. As a result, surface air temperature rises over NC (Fig. 8h). The

reduced latent heat flux is particularly evident in the canopy evaporation in the NC region (Fig. 9d), although there is also reduced soil evaporation during the summer (Fig. 9a).

Similarly, surface cooling over SC and KR is considered in summer. Broadleaf tree fraction expansion (Fig. 8b) increases the roughness length (Fig. 8f) and latent heat flux (Fig. 8c), driving surface cooling. While the NC region, where bare soil fraction is increased, showed a decrease of evaporation from A to AE, in the KR and SC regions where broadleaf tree fraction is increased there is increased soil and canopy evaporation from A to AE (Fig. 9). These results are consistent with the suggestion by Lee et al. (2011) that a vegetation replacement with bare soil would cause an associated decrease in latent heat during the summer. In summary, for the present climate, the land cover effect (bare soil fraction changes in Fig. 8a) is related to surface air temperature changes in summer (Fig. 8h). As soil fraction expands (shrinks) the temperature rises (drops).

As regards precipitation, Fig. 6 shows only very small changes in precipitation over land in AEnod-Anod (Fig. 6b). Thus, the model's direct sensitivity of precipitation to changes in land surface conditions seems to be low compared with the sensitivity to the dust changes that result from them.

3.1.3 Impact of dust radiative feedback

We now consider the direct radiative effect of dust resulting from the changes in the vegetation distribution (AEnod – Anod and AE – AEnod of Fig. 10). Concerning the regional climate response, the dust direct radiative effects (Fig. 10b) are represented by anomalous northeasterly coastal flow counteracting the summertime climatological monsoonal circulation associated with the western North Pacific high, known to be important in the East Asian summer monsoon rainfall (Lee et al., 2006, and Fig. 10c). The sea level pressure and wind anomalies in "AE – AEnod" are stronger than those of "AEnod – Anod" (Fig. 10a and b), illustrating that the radiative effects of the dust have a larger impact than the surface vegetation changes themselves.

The direct radiative effect of dust induces anomalous cyclonic flow over the western North Pacific (KR region in Fig. 10b) that would tend to decrease rainfall over East Asian continent. This is because dust reflects a considerable amount of shortwave radiation, as shown by the increase of upward shortwave radiation at the top of atmosphere (TOA; Fig. 10f), with a resulting cooling the land surface (Fig. 10d). The land surface cooling appears on the continental scale. This is somewhat different from the results in Miller and Tegen (1998) in which they mentioned that the reflected solar flux is offset by the absorption of upwelling longwave radiation, so that the net radiation entering the TOA is only weakly perturbed by dust in comparison to the surface reduction. Although the upward longwave flux is reduced through the dust radiative effects (Fig. 10e), the reduction is smaller than the increase in reflected shortwave at the TOA. Differential heating between land and ocean is one of the fundamental driving mechanisms of the monsoon (Webster et al., 1998). The land–sea thermal contrast becomes weaker due to the direct radiative effect of dust and the pressure contrast weakens. Strong anomalous northeasterly flow along the coast (Fig. 10b), weakening the summer monsoon inflow, induces the dry bias over SC and KR (Fig. 6c). These results seem in line with the argument that dust-induced surface cooling is the dominant mechanism leading to a reduction of precipitation (Konaré et al., 2008; Yoshioka et al., 2007; Paeth and Feichter, 2005).

3.2 Future experiments

The effect of including a DGVM, particularly with the feedback on the dust loading, is expected to affect the simulation of future climate change. Changes in AEts relative to AE show increases in rainfall over SC, KR and the western North Pacific (Fig. 11b). Compared with differences between Ats and A in Fig. 11a and b shows a further reduction in rainfall over the South China Sea (SCS) to the south of 20° N accompanied by anticyclonic flow at 850 hPa. The discrepancy in future changes in precipitation tends to be larger than that of temperature: Fig. 11c and d present similar warming patterns.

In order to examine the role of different vegetation distributions in global warming, with and without the dust feedbacks, we analyze future timeslice experiments in a similar manner to ML12. To estimate individually the impact of land cover, feedback on the dust loading, and climate change of global warming, we use the experiments described in Table 2. Note that "Dust" and "LCC" are "double differences" illustrating the impacts of the inclusion of the land cover changes, and the radiative effects of the dust changes that the land cover change induces, on the future – present differences.

According to Baek et al. (2013), the warming and rainfall increment from RCP8.5 are expected to be of the order of 6 ± 1 K and 17 % over East Asia. The temperature rises in the timeslice experiments are of similar magnitude (Figs. 11c, d and 12b). Precipitation is anticipated to increase by 10–15 % toward the end of the 21st century over the major monsoonal front region over East Asia in good CMIP5 models simulations under the RCP6.0 scenario (Seo et al., 2013). Consistent with this, Figs. 11 and 12 project a warmer and wetter climate in future summer over NC, KR and SC. Figures 11b and 12a show that a larger increase in rainfall between future and present timeslice run is simulated in these regions when land cover change and feedback on the dust are included. However, while precipitation changes over the SCS region tend to be slightly positive on average in climate change-only, including land cover changes and feedback with dust induces a reduction in rainfall in this region.

The land surface cover differences in this region between future and present-day climate projected by this model are in C_3 grass expansion replacing bare soil (Fig. 13c and f). These changes contribute increases in the evaporation and latent heat flux and decreases in surface air temperature (Fig. 14a and b) to the overall future – present changes. Comparison between (AEnodts – AEnod) and (Ats – A) in Fig. 11 showed that the changes in land cover contribute to increased rainfall over the land and reduced rainfall over the SCS. Increasing latent heat flux accompanies lower boundary layer height and is associated with boundary layer moistening (Fig. 14c). According to Lee et al. (2009, 2011), a more vegetated surface tends to be associated with surface moistening, favoring an increase in latent heat and atmospheric moisture (Fig. 14).

The changes in vegetation and associated changes in surface air temperature, latent heat fluxes (Fig. 14a and b) and low level circulation (Fig. 14d) are in a similar pattern, but opposite sign, to those shown in Figs. 7b, 8c and 10a. This suggests that the future differences between experiments with different land cover (AEnodts – Ats) are small compared with the present-day differences (AEnod – A) such that the double-difference (AEnodts – AEnod) – (Ats – A) is dominated by the present-day differences. This is consistent with the findings of ML12.

In Fig. 14d, increased rainfall over the SC region from 25 to 35° N is associated with additional anomalous convergence and upward motion over the SC region (see Fig. 15a) induced by the land cover change effect as the monsoon differential circulation results in enhanced moisture transport and cloud formation over SC and KR. In contrast, over the SCS, anomalous anticyclonic flow is related to downward motion from 10 to 20° N (Fig. 15a) and reduced rainfall (Fig. 14d).

As shown in Fig. 12a, the dust radiative forcing is the main contributor to the reduction of simulated precipitation over SCS to the south of 20° N in the AEts future experiment. Figure 16 shows the double-difference (AEts minus AE) minus (AEnodts minus AEnod). The atmospheric response of Fig. 16 seems to be largely opposite to that in Fig. 10b, e and f, suggesting that it is dominated by the present-day impacts of dust seen between AE and AEnod. In global warming (i.e. future – present), the bare soil fraction decreases (Fig. 13f) so the dust emission of HadGEM2-ES decreases in the future relative to the present climate (Fig. 17). As mentioned in Sect. 3.1.3, the direct radiative effect of dust seems to induce stronger flow than that of ES land cover-only effect. The convective region over SC in the future experiment Ats (Figs. 11a and 15c) is strengthened in AEts (Fig. 11b), and that over the SCS weakened, through the radiative effects of the reduced dust loading (Fig. 15b), with related increases and decreases in precipitation (Figs. 16d and 12a).

Overall, for future precipitation projection over East Asia using this model, simulating interactive land cover change by a DGVM, and particularly the subsequent changes in dust radiative effect, are at least as important as the warming conditions. In contrast,

for future changes in temperature, the global warming effect is dominant among climate change, land cover change and dust radiative effects over East Asia (Figs. 11c, d and 12b).

4   Summary and discussion

In this study, the impact of varying land cover distribution, as simulated by a DGVM, on simulated regional climate over East Asia is examined. The interaction between land cover change by the DGVM and model systematic biases are shown in the present-day climate. The climatology of HadGEM2-A has an underestimation of rainfall over KR in summer and an overestimation over SC. When the land cover from HadGEM2-ES, which uses an interactive vegetation model, is used as an input to HadGEM2-A (experiment AE), the precipitation bias is enhanced over KR and SCS. The difference between AE and A is related to regional bare soil expansion by the DGVM through interaction with the rainfall bias, and also through feedback with the subsequent dust loading, causing a direct radiative effect. The direct radiative effect of dust has an important influence on both the precipitation bias and the stronger circulation response in SLP and wind than the land cover-only effect does. In this study, more dust loading due to excessive bare soil fraction induces an amplified dry bias over Asia. The land cover difference between AE and A affects the surface air temperature bias. In summer, a warm bias in NC (Fig. 8h) is due to bare soil area expansion replacing vegetation (Fig. 8). Soil fraction expands (shrinks) and temperature rises (drops) over NC (SC) (Fig. 8) through changes in surface roughness, evaporation and latent heat fluxes.

The dust loading is expected to reduce in the future time-slice run, since C_3 grass replaces bare soil area over NC. The consequent direct radiative effect of dust changes induces the opposite direction of anomalous wind flow over the SCS compared with that induced by the CO_2 increase alone. Thus, in the future projection, suppressed rainfall appears over the SCS. Just as the direct radiative effect is significant in the future precipitation simulation, the land cover effect is also important. The C_3 grass expansion

replacing bare soil, inducing an increase in latent heat flux, lowers the surface temperature. The changes in land cover between future and present day tend to oppose the surface warming over NC and KR in summer that are driven by increasing CO_2 in the time-slice experiments. When the land cover change impacts and associated dust radiative effect are combined, the resulting rainfall under future climate differs regionally. In contrast with the precipitation response, the temperature response in the time-slice run is dominated by the warming induced from the atmospheric CO_2 increase. In terms of the projected temperature rise, the ES land cover and dust radiative effects are very small. Overall, the inclusion of land cover changes as simulated by an interactive vegetation model has impacts on both present and future climate in East Asia. These results are similar to those for India shown in ML12, although the response amplitude is different.

Inclusion of dynamic vegetation components in a climate model allows impacts of climate change on both atmospheric composition and ecosystems. When the various feedbacks among the model components are included, complexity increases and the feedbacks affect more numerous systematic biases in models and future climate projections (ML12). ML12 mentioned that, as Earth System process are included in a model, the systematic biases need to be studied in order to understand how additional feedbacks from the interactive components in Earth system models affect climate projection. Although the details of our results may be dependent on the particular modelling system used for this study, nevertheless they suggest that vegetation feedbacks may be important over East Asia, particularly in the dust emission source regions, for present-day and future climate simulation.

References

Adler, R. F., Huffman, G. J., Chang, A., Ferraro, R., Xie, P., Janowiak, J., Rudolf, B., Schnei-der, U., Curtis, S., Bolvin, D., Gruber, A., Susskind, J., Arkin, P., and Nelkin, E.: The Version 2 Global Precipitation Climatology Project (GPCP) monthly precipitation analysis (1979–present), J. Hydrometeorol., 4, 1147–1167, 2003.

Baek, H.-J., Lee, J., Lee, H.-S., Cho, C., Kwon, W.-T., Marzin, C., Hyun, Y.-K., Gan, S.-Y., Kim, M.-J., Choi, D.-H., Lee, J., Lee, J., Boo, K.-O., Kang, H.-S., and Byun, Y.-H.: Climate change in the 21st century simulated by HadGEM2-AO under representative concentration pathways, Asia-Pac. J. Atmos. Sci., 49, 603–618, 2013.

Batlle Bayer, L., van den Hurk, B. J. J. M., Strengers, B. J., and van Minnen, J. G.: Regional feedbacks under changing climate and land-use conditions, Earth Syst. Dynam. Discuss., 3, 201–234, doi:10.5194/esdd-3-201-2012, 2012.

Collins, W. J., Bellouin, N., Doutriaux-Boucher, M., Gedney, N., Halloran, P., Hinton, T., Hughes, J., Jones, C. D., Joshi, M., Liddicoat, S., Martin, G., O'Connor, F., Rae, J., Senior, C., Sitch, S., Totterdell, I., Wiltshire, A., and Woodward, S.: Development and evaluation of an Earth-System model – HadGEM2, Geosci. Model Dev., 4, 1051–1075, doi:10.5194/gmd-4-1051-2011, 2011.

Cox, P. M.: Description of the "TRIFFID" Dynamic Global Vegetation Model, Hadley Centre Technical Note No. 24, Met Office Hadley Centre, Exeter, UK, available at: http://www.metoffice.gov.uk/media/pdf/9/h/HCTN_24.pdf (last access: 15 October 2014), 2001.

Cox, P. M., Betts, R. A., Bunton, C. B., Essery, R. L. H., Rowntree, P. R., and Smith, J.: The impact of new land surface physics on the GCM simulation of climate and climate sensitivity, Clim. Dynam., 15, 183–203, doi:10.1007/s003820050276, 1999.

Douglas, E. M., Niyogi, D., Frolking, S., Yeluripati, J. B., Pielke Sr., R. A., Niyogi, N., Vorosmarty, C. J., and Mohanty, U. C.: Changes in moisture and energy fluxes due to agricultural land use and irrigation in the Indian Monsoon Belt, Geophys. Res. Lett., 33, L14403, doi:10.1029/2006GL026550, 2006.

Essery, R. and Clark, D. B.: Developments in the MOSES 2 land-surface model for PILPS 2e, Global Planet. Change, 38, 161–164, doi:10.1016/j.bbr.2011.03.031, 2003.

Harris, I., Jones, P. D., Osborn, T. J., and Lister, D. H.: Updated high-resolution grids of monthly climatic observations – the CRU TS3.10 Dataset, Int. J. Climatol., 34, 623–642, doi:10.1002/joc.3711, 2013.

Title Page

Abstract | Introduction

Conclusions | References

Tables | Figures

|◄ | ►|

◄ | ►

Back | Close

Full Screen / Esc

Printer-friendly Version

Interactive Discussion

Huffman, G. J., Adler, R. F., Bolvin, D. T., and Gu, G.: Improving the global precipitation record: GPCP version 2.1, Geophys. Res. Lett., 36, L17808, doi:10.1029/2009GL040000, 2009.

Hurrell, J., Meehl, G. A., Bader, D., Delworth, T. L., Kirtman, B., and Wielicki, B.: A unified modeling approach to climate system prediction, B. Am. Meteorol. Soc., 90, 1819–1832, doi:10.1175/2009BAMS2752.1, 2009.

Hurtt, G. C., Chini, L. P., Frolking, S., Betts, R., Feddema, J., Fischer, G., Fisk, J. P., Hibbard, K., Houghton, R. A., Janetos, A., Jones, C., Kindermann, G., Kinoshita, T., Klein Goldewijk, K.,Riahi, K., Shevliakova, E., Smith, S., Stehfest, E., Thomson, A., Thornton, P., van Vuuren, D. P., and Wang, Y.: Harmonization of land-use scenarios for the period 1500–2100: 600 years of global gridded annual land-use transitions, wood harvest, and resulting secondary lands, Climatic Change, 109, 117–161, doi:10.1007/s10584-011-0153-2, 2011.

Jones, C. D., Hughes, J. K., Bellouin, N., Hardiman, S. C., Jones, G. S., Knight, J., Liddicoat, S., O'Connor, F. M., Andres, R. J., Bell, C., Boo, K.-O., Bozzo, A., Butchart, N., Cadule, P., Corbin, K. D., Doutriaux-Boucher, M., Friedlingstein, P., Gornall, J., Gray, L., Halloran, P. R., Hurtt, G., Ingram, W. J., Lamarque, J.-F., Law, R. M., Meinshausen, M., Osprey, S., Palin, E. J., Parsons Chini, L., Raddatz, T., Sanderson, M. G., Sellar, A. A., Schurer, A., Valdes, P., Wood, N., Woodward, S., Yoshioka, M., and Zerroukat, M.: The HadGEM2-ES implementation of CMIP5 centennial simulations, Geosci. Model Dev., 4, 543–570, doi:10.5194/gmd-4-543-2011, 2011.

Kang, H.-S. and Hong, S.-Y.: An assessment of the land surface parameters on the simulated regional climate circulations: the 1997 and 1998 east Asian summer monsoon cases, J. Geophys. Res., 113, D15121, doi:10.1029/2007JD009499, 2008.

Kang, H.-S., Cha, D.-H., and Lee, D.-K.: Evaluation of the mesoscale model/land surface model (MM5/LSM) coupled model for East Asian summer monsoon simulations, J. Geophys. Res., 110, D10105, doi:10.1029/2004JD005266, 2005.

Konaré, A., Zakey, A. S., Solmon, F., Giorgi, F., Rauscher, S., Ibrah, S., and Bi, X.: A regional climate modeling study of the effect of desert dust on the West African monsoon, J. Geophys. Res., 113, D12206, doi:10.1029/2007JD009322, 2008.

Lau, K. M. and Kim, K.-M.: Observational relationships between aerosol and Asian monsoon rainfall, and circulation, Geophys. Res. Lett., 33, L21810, doi:10.1029/2006GL027546, 2006.

Lau, K. M. and Li, M.-T.: The monsoon of East Asia and its global associations – a survey, B. Am. Meteorol. Soc., 65, 114–125, 1984.

Title Page

Abstract | Introduction

Conclusions | References

Tables | Figures

◄ | ►

◄ | ►

Back | Close

Full Screen / Esc

Printer-friendly Version

Interactive Discussion

Lau, K. M., Kim, M. K., and Kim, K. M.: Asian monsoon anomalies induced by aerosol direct effects, Clim. Dynam., 26, 855–864, doi:10.1007/s00382-006-0114-z, 2006.

Lawrence, D. M. and Slingo, J. M.: An annual cycle of vegetation in a GCM, Part I: Implementation and impact on evaporation, Clim. Dynam., 22, 87–105, doi:10.1007/s00382-003-0366-9, 2004.

Lee, E., Chase, T. N., Rajagopalan, B., Barry, R. G., Biggs, T. W., and Lawrence, P. J.: Effects of irrigation and vegetation activity on early Indian summer and monsoon variability, Int. J. Climatol., 29, 573–581, doi:10.1002/joc.1721, 2009.

Lee, E., Barford, C. C., Kucharik, C. J., Felzer, B. S., and Foley, J. A.: Role of turbulent heat fluxes over land in the monsoon over East Asia, Int. J. Geosci., 2, 420–431, doi:10.4236/ijg.2011.24046, 2011.

Lee, E. J., Yeh, S. W., Jhun, J. G., and Moon, B. K.: Seasonal change in anomalous WNPSH associated with the strong East Asian summer monsoon, Geophys. Res. Lett., 33, L21702, doi:10.1029/2006GL027474, 2006.

Loveland, T. R., Reed, B. C., Brown, J. F., Ohlen, D. O., Zhu, Z., Yang, L., and Merchant, J. W.: Development of a global land cover characteristics database and IGBP DISCover from 1 km AVHRR data, Int. J. Remote Sens., 21, 1303–1330, doi:10.1080/014311600210191, 2000.

Martin, G. M. and Levine, R. C.: The influence of dynamic vegetation on the present-day simulation and future projections of the South Asian summer monsoon in the HadGEM2 family, Earth Syst. Dynam., 3, 245–261, doi:10.5194/esd-3-245-2012, 2012.

McCarthy, M. P., Sanjay, J., Booth, B. B. B., Krishna Kumar, K., and Betts, R. A.: The influence of vegetation on the ITCZ and South Asian monsoon in HadCM3, Earth Syst. Dynam., 3, 87–96, doi:10.5194/esd-3-87-2012, 2012.

Miller, R. L. and Tegen, I.: Climate response to soil dust aerosols, J. Climate, 11, 3247–3267, 1998.

Paeth, H. and Feichter, J.: Greenhouse-gas versus aerosol forcingand African climate response, Clim. Dynam., 26, 35–54, 2005.

Qian, Y., Gong, D., Fan, J., Leung, L. R., Bennartz, R., Chen, D., and Wang, W.: Heavy pollution suppresses light rain in China: observations and modeling, J. Geophys. Res., 114, D00K02, doi:10.1029/2008JD011575, 2009.

Title Page

Abstract | Introduction

Conclusions | References

Tables | Figures

|◄ | ►|

◄ | ►

Back | Close

Full Screen / Esc

Printer-friendly Version

Interactive Discussion

Ramanathan, V., Chung, C., Kim, D., Betge, T., Buja, L., Kiehl, J. T., Washington, W. M., Fu, Q., Sikka, D. R., and Wild, M.: Atmospheric brown clouds: impacts on South Asian climate and hydrological cycle, P. Natl. Acad. Sci. USA, 102, 5326–5333, doi:10.1073/pnas.0500656102, 2005.

Seo, K.-H. O., Ok, J., Son, J.-H., and Cha, D.-H.: Assessing future changes in the East Asian summer monsoon using CMIP5 coupled Models, J. Climate, 26, 7662–7675, doi:10.1175/JCLI-D-12-00694.1, 2013.

Sokolik, I. N. and Toon, O. B.: Direct radiative forcing by anthropogenic airborne mineral aerosols, Nature, 381, 681–683, 1996.

Suh, M.-S. and Lee, D.-K.: Impacts of land use/cover changes on surface climate over east Asia for extreme climate cases using RegCM2, J. Geophys. Res., 109, D02108, doi:10.1029/2003JD003681, 2004.

Taylor, K. E., Stouffer, R. J., and Meehl, G. A.: An overview of CMIP5 and the experiment design, B. Am. Meteorol. Soc., 93, 485–498, doi:10.1175/BAMS-D-11-00094.1, 2012.

The HadGEM2 Development Team: G. M. Martin, Bellouin, N., Collins, W. J., Culverwell, I. D., Halloran, P. R., Hardiman, S. C., Hinton, T. J., Jones, C. D., McDonald, R. E., McLaren, A. J., O'Connor, F. M., Roberts, M. J., Rodriguez, J. M., Woodward, S., Best, M. J., Brooks, M. E., Brown, A. R., Butchart, N., Dearden, C., Derbyshire, S. H., Dharssi, I., Doutriaux-Boucher, M., Edwards, J. M., Falloon, P. D., Gedney, N., Gray, L. J., Hewitt, H. T., Hobson, M., Huddleston, M. R., Hughes, J., Ineson, S., Ingram, W. J., James, P. M., Johns, T. C., Johnson, C. E., Jones, A., Jones, C. P., Joshi, M. M., Keen, A. B., Liddicoat, S., Lock, A. P., Maidens, A. V., Manners, J. C., Milton, S. F., Rae, J. G. L., Ridley, J. K., Sellar, A., Senior, C. A., Totterdell, I. J., Verhoef, A., Vidale, P. L., and Wiltshire, A.: The HadGEM2 family of Met Office Unified Model climate configurations, Geosci. Model Dev., 4, 723–757, doi:10.5194/gmd-4-723-2011, 2011.

Webster, P. J., Magana, V. O., Palmer, T. N., Shukla, J., Tomas, R. A., Yanai, M., and Yasunari, T.: Monsoons: processes, predictability, and the prospects for prediction, J. Geophys. Res., 3, 14451–14510, doi:10.1029/97JC02719, 1998.

Xie, P. and Arkin, P. A.: Global precipitation: a 17-year monthly analysis based on gauge observations, satellite estimates, and numerical model outputs, B. Am. Meteorol. Soc., 78, 2539–2558, 1997.

Yamashima, R., Takata, K., Matsumoto, J., and Yasunari, T.: Numerical study of the impacts of land use/cover changes between 1700 and 1850 on the seasonal hydroclimate in monsoon Asia, J. Meteorol. Soc. Jpn., 89A, 291–298, doi:10.2151/jmsj.2011-A19, 2011.

Yoshioka, M., Mahowald, N. M., Conley, A. J., Collins, W. D., Fillmore, D. W., Zender, C. S., and Coleman, D. B.: Impact of desert dust radiative forcing on Sahel precipitation: relative importance of dust compared to sea surface temperature variations, vegetation changes, and greenhouse gas warming, J. Climate, 20, 1445–1467, doi:10.1175/JCLI4056.1, 2007.

The impact of land cover generated by a dynamic vegetation model on climate over East Asia

M.-H. Cho et al.

Table 1. List of experiments.

Acronym	Description of the experiments	Time
A	HadGEM2-A	Present
AE	HadGEM2-A with ES vegetation	1980–
Anod	HadGEM2-A with no dust radiative effects	2005
AEnod	HadGEM2-A with ES vegetation with no dust radiative effects	
Ats	HadGEM2-A time slice run	Future
AEts	HadGEM2-A with ES vegetation time slice run	2080–
AEnodts	HadGEM2-A with ES vegetation time slice run with no dust radiative effects	2110

Title Page

Abstract | Introduction

Conclusions | References

Tables | Figures

|◄ | ►|

◄ | ►

Back | Close

Full Screen / Esc

Printer-friendly Version

Interactive Discussion

Table 2. Impacts of climate change of global warming, land cover change and dust loading obtained by the difference between the experiments in this study.

Impact	Descriptions
Climate change (Global warming)	Ats – A
Climate change + LCC + Dust	AEts – AE
Climate change + LCC	AEnodts – AEnod
Dust	(AEts – AE) – (AEnodts – AEnod)
LCC (ES land cover)	(AEnodts – AEnod) – (Ats – A)

Figure 1. The 1982–2005 **(a)** climatology of the Global Precipitation Climatology Project (GPCP) precipitation (mm day^{-1}, shading) and 850 hPa winds (m s^{-1}) and **(b)** precipitation difference between GPCP and the CPC Merged Analysis of Precipitation (CMAP) in JJA.

Figure 2. Area averaged precipitation bias (mm day^{-1}) compared to observation in JJA: **(a)** and **(b)** show regional mean biases over the regions shown in **(c)** and **(d)**. NC region: 35–50° N, 105–120° E; KR: 25–40° N, 120–135° E; SC region: 20–35° N, 105–120° E.

Title Page

Abstract | Introduction

Conclusions | References

Tables | Figures

|◄ | ►|

◄ | ►

Back | Close

Full Screen / Esc

Printer-friendly Version

Interactive Discussion

Figure 3. As Fig. 2 but for JJA surface air temperature biases (K) compared to the Climatic Research Unit (CRU) climatology.
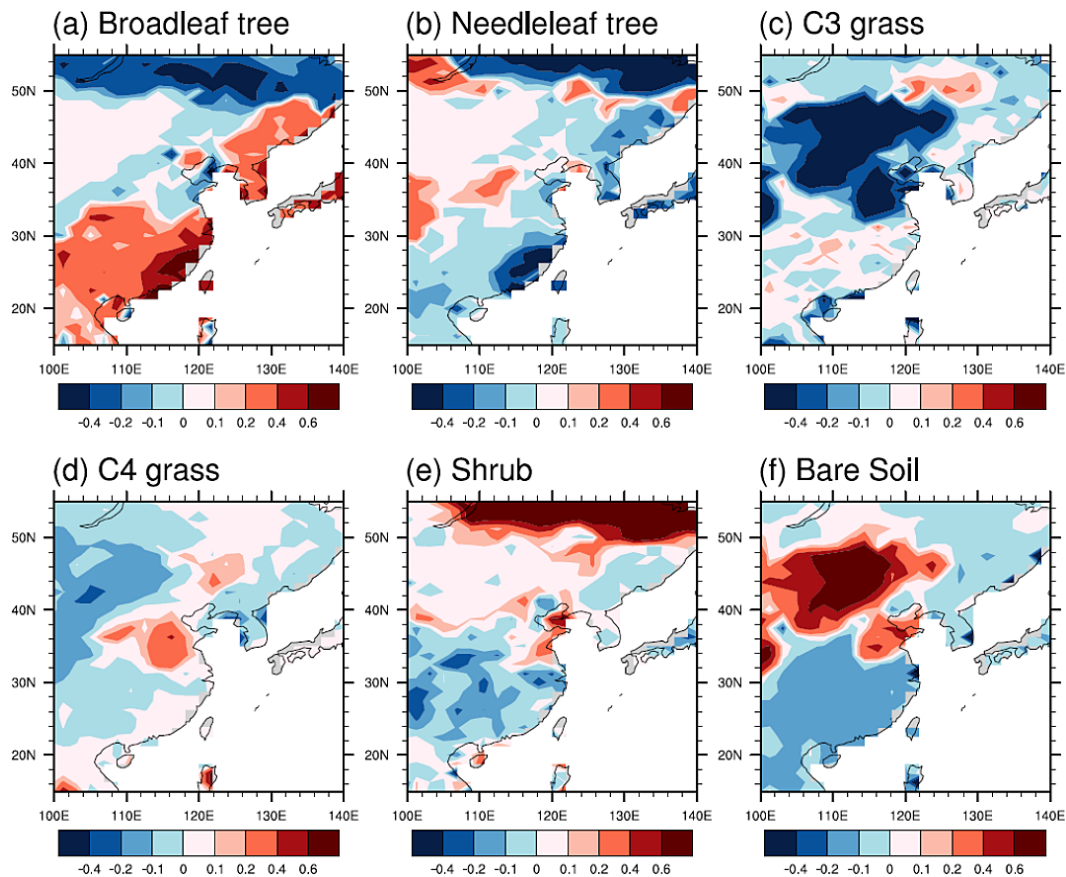
Figure 4. Differences in present-day (1980–2005) fractions of land cover type between HadGEM2-ES and HadGEM2-AO (and HadGEM2-A) over East Asia.
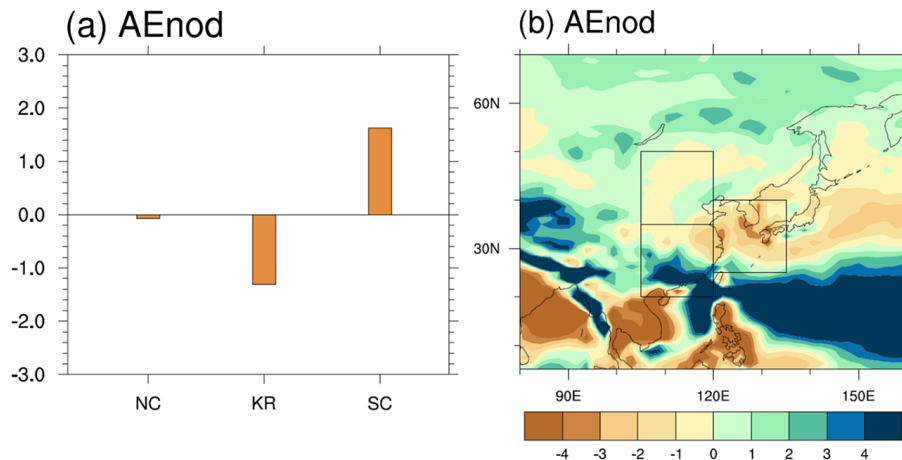
Figure 5. Summer **(a)** area averaged precipitation bias ($\mathrm{mm\,day^{-1}}$) compared to observation and **(b)** horizontal distribution of precipitation bias, in AE simulation without the direct radiative effect of dust.
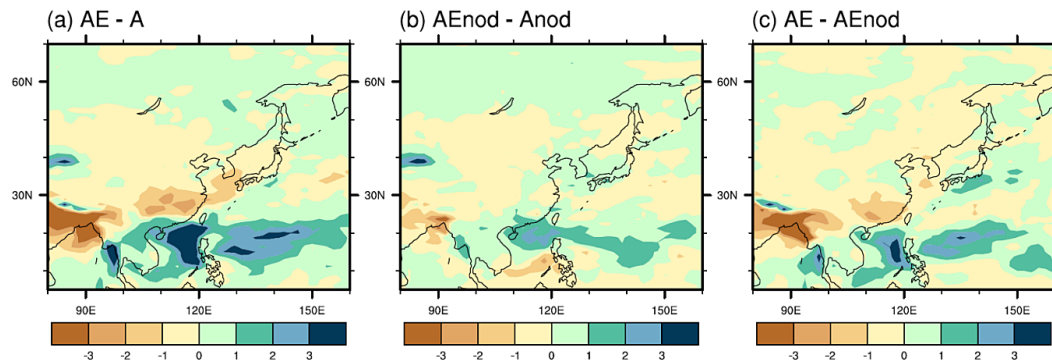
Figure 6. Precipitation differences (mm day^{-1}) in summer for **(a)** AE minus A **(b)** AEnod minus Anod, and **(c)** AE minus AEnod.
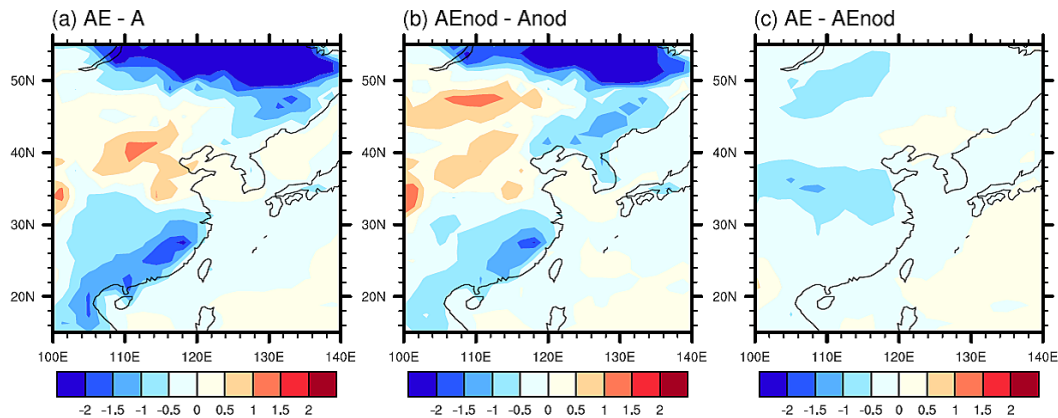
Figure 7. Surface air temperature differences (K) in JJA for **(a)** AE minus A, **(b)** AEnod minus Anod, **(c)** AE minus AEnod.
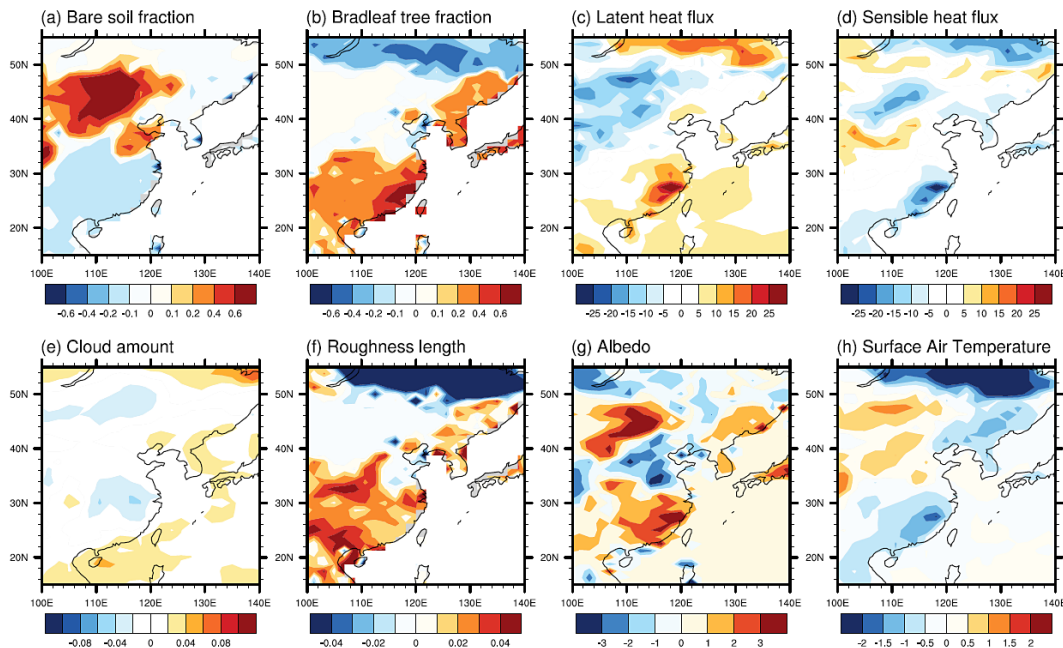
Figure 8. AEnod minus Anod in JJA showing the applied fractional land cover changes and their impact in **(a)** bare soil fraction, **(b)** broadleaf tree fraction, **(c)** latent heat flux (W m^{-2}), **(d)** sensible heat flux (W m^{-2}), **(e)** cloud amount (fraction), **(f)** roughness length (m), **(g)** albedo (%) and **(h)** surface air temperature (K).
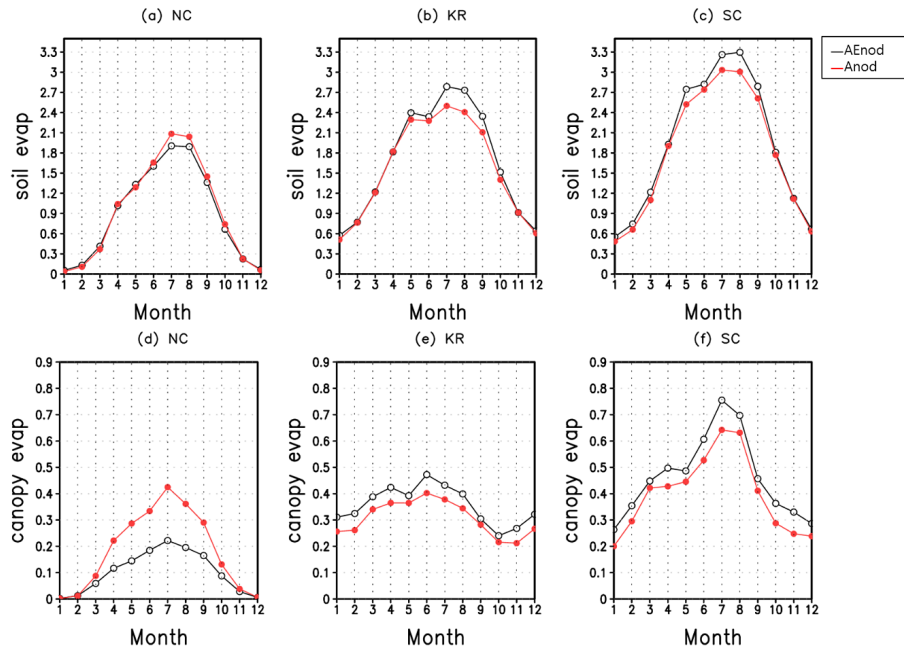
Figure 9. Monthly variation of soil and canopy evaporation ($mm\,day^{-1}$) in AEnod and Anod for the present-day simulation (1982–2005) over North China (NC), Korea (KR), South China (SC) region.
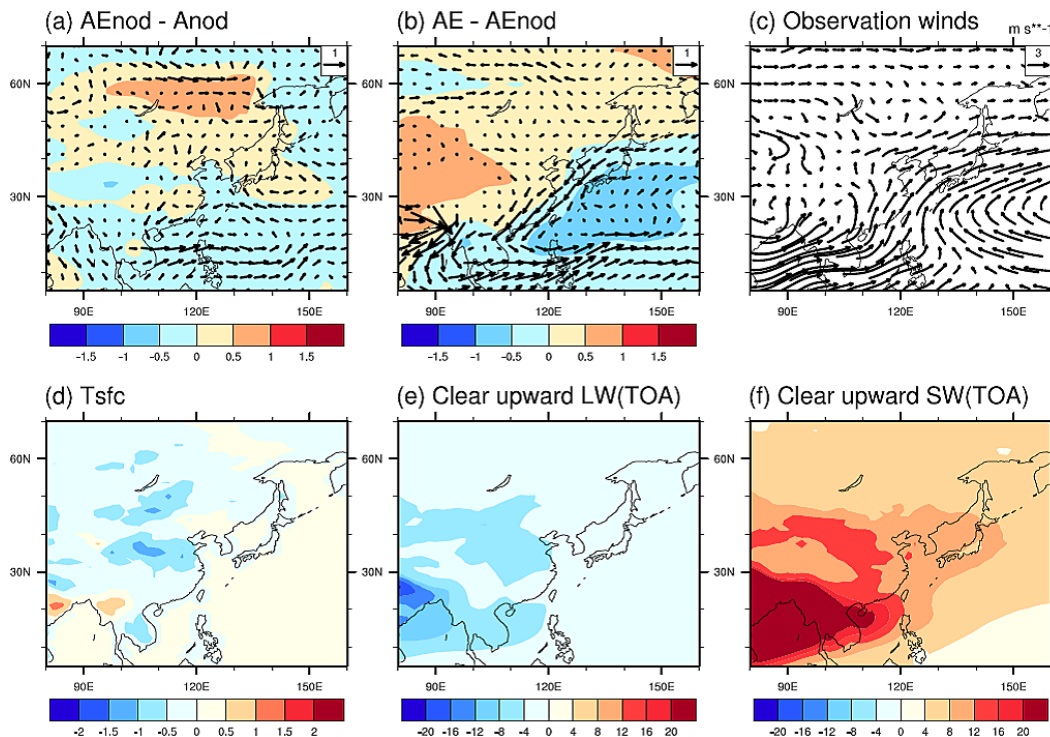
Figure 10. Changes in mean sea level pressure (hPa) and 850 hPa winds (m s^{-1}) in JJA for **(a)** AEnod minus Anod, and **(b)** AE minus AEnod. **(c)** Climatology of 850 hPa winds for the period 1982–2005 using ERA Interim; **(d)**–**(f)** show differences between AE and AEnod in JJA: **(d)** surface temperature (K), **(e)** clear sky upward longwave radiation (W m^{-2}) and **(f)** clear sky upward shortwave radiation (W m^{-2}) at top of atmosphere, showing the impacts of the radiative effects from additional dust loading induced by the ES land cover.
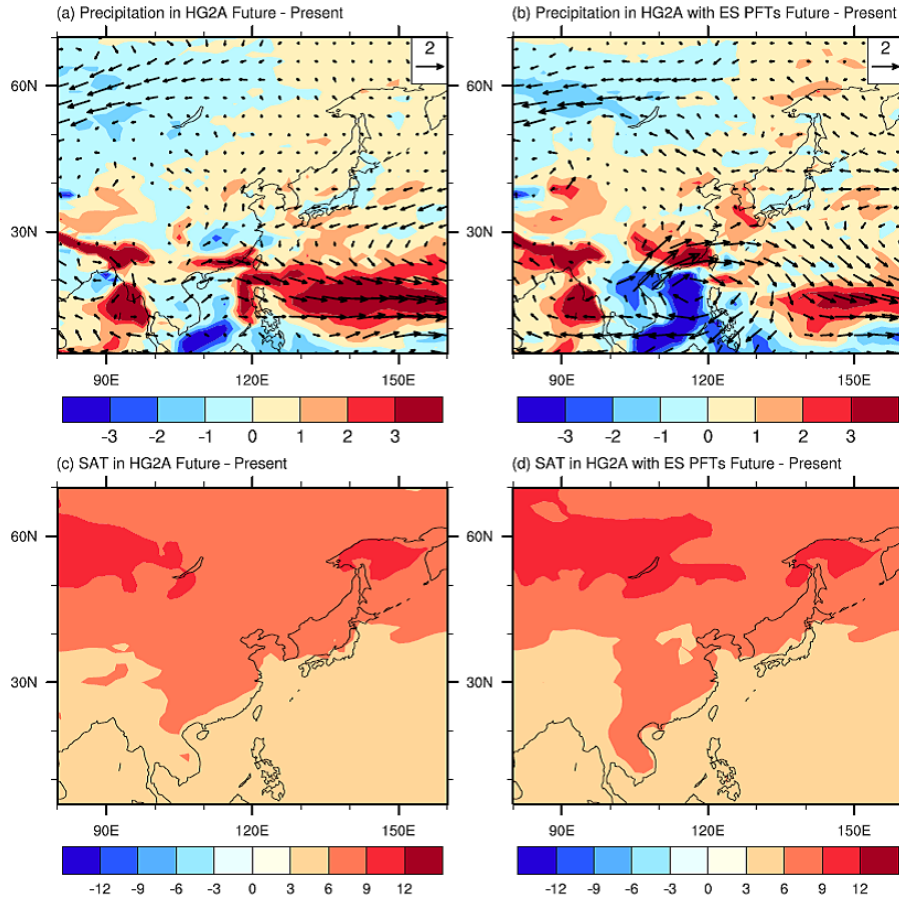
Figure 11. Changes in JJA mean precipitation (shading, $\mathrm{mm\,day^{-1}}$) between future timeslice and present-day HadGEM2-A experiments, without **(a)**, **(c)** and with **(b)**, **(d)** land cover from HadGEM2-ES. **(a)**, **(c)** is (Ats – A) and **(b)**, **(d)** is (AEts – AE).
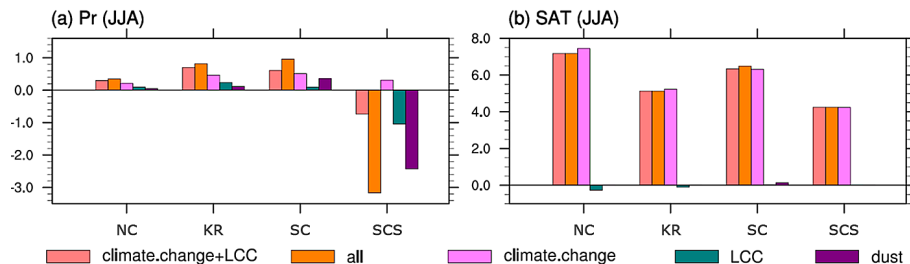
Figure 12. Future changes of precipitation (mm day^{-1}) **(a)** and surface air temperature (K) **(b)** over the box regions of North China (NC), Korea (KR), South China (SC) and South China Sea (SCS) in summer. Note that "all" means sum of climate change, land cover change and direct radiative effect of dust; "LCC" and "Dust" are "double-differences" illustrating the influence of those processes on the future – present changes.
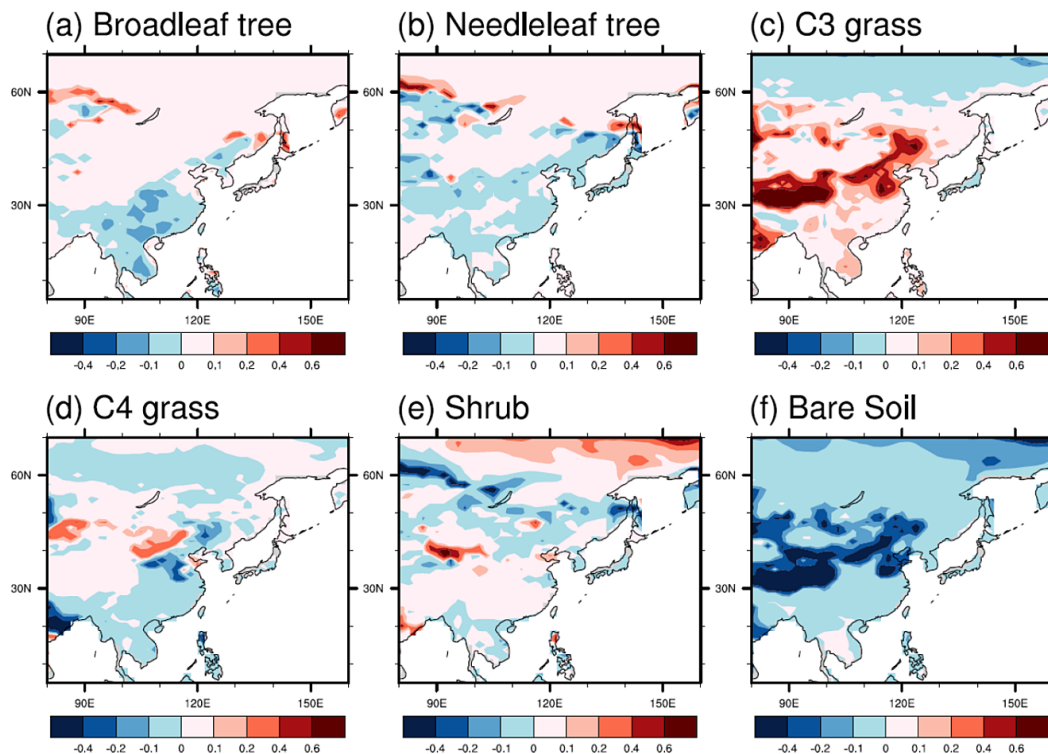
Figure 13. Changes of fractions in land cover between c.2100 and present-day as simulated by HadGEM2-ES in the Fifth Coupled Model Intercomparison Project (CMIP5) the Representative Concentration Pathway (RCP) 8.5 scenario and applied in AE present and AEts future time-slice experiments.
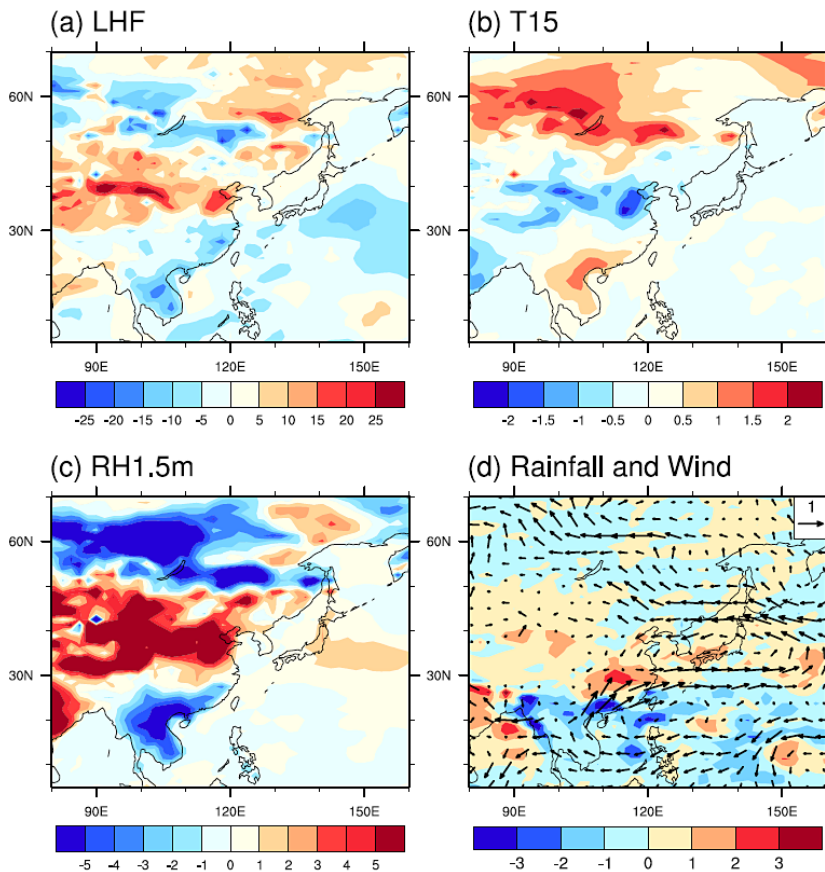
Figure 14. Contribution by the land cover changes alone to the future – present differences in summer (represented by (AEnodts – AEnod) – (Ats – A)) in **(a)** latent heat flux (W m^{-2}), **(b)** surface air temperature (K), **(c)** 1.5 m relative humidity (%) and **(d)** rainfall (shading, mm day^{-1}), 850 hPa wind (vectors, m s^{-1}).
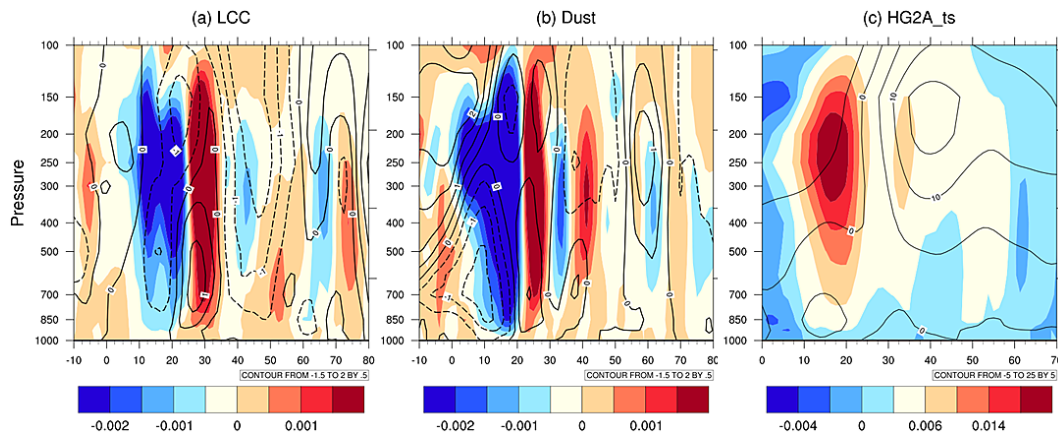
Figure 15. (a) and **(b)** Contribution to future – present changes in vertical motion (upward: red, downward: blue) and U wind anomalies (solid line: westerlies) from 110–120° E driven by **(a)** LCC impact, and **(b)** dust impact. **(c)** Climatological vertical motion over 110–120° E in the HadGEM2-A timeslice run, Ats.
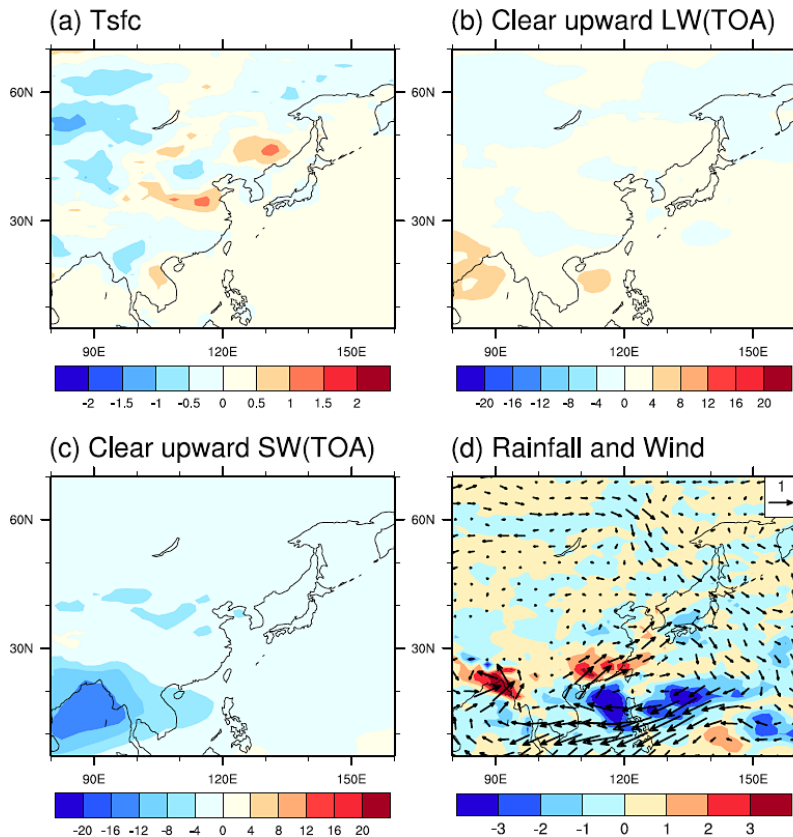
Figure 16. As Fig. 14 but showing the contribution from the direct radiative effect of dust to the future – present differences (represented by (AEts – AE) – (AEnodts – AEnod)) in JJA in **(a)** surface temperature (K), **(b)** clear sky upward longwave radiation at top of atmosphere (W m^{-2}), **(c)** clear sky upward shortwave radiation at top of atmosphere (W m^{-2}) and **(d)** rainfall (shading, mm day^{-1}), 850 hPa wind (vectors, m s^{-1}).
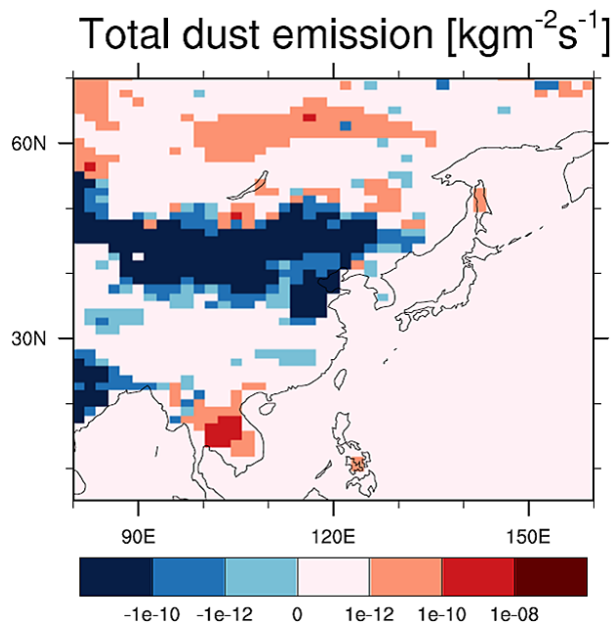
Figure 17. Future changes in total dust emission ($kg\,m^{-2}\,s^{-1}$) in JJA from AEts – AE.